

$O(4)$ -symmetric position-space renormalization of lattice operators

Masaaki Tomii^{1,*} and Norman H. Christ¹

¹*Physics Department, Columbia University, New York 10027, USA*

Abstract

We extend the position-space renormalization procedure, where renormalization factors are calculated from Green's functions in position space, by introducing a technique to take the average of Green's functions over spheres. In addition to reducing discretization errors, this technique enables the resulting position-space correlators to be evaluated at any physical distance, making them continuous functions similar to the $O(4)$ -symmetric position-space Green's functions in the continuum theory but with a residual dependence on a regularization parameter, the lattice spacing a . We can then take the continuum limit of these renormalized quantities calculated at the same physical renormalization scale $|x|$ and investigate the resulting $|x|$ -dependence to identify the appropriate renormalization window.

As a numerical test of the spherical averaging technique, we determine the renormalized light and strange quark masses by renormalizing the scalar current. We see a substantial reduction of discretization effects on the scalar current correlator and an enhancement of the renormalization window. The numerical simulation is carried out with $2 + 1$ -flavor domain-wall fermions at three lattice cutoffs in the range 1.79–3.15 GeV.

* mt3164@at.columbia.edu

I. INTRODUCTION

Operator renormalization is necessary to calculate many quantities such as weak matrix elements using lattice simulation. So far, several different methods to renormalize lattice operators have been proposed, applied and improved. Since each method has individual advantages and disadvantages, we can use the method that is the most convenient for our situation and purpose.

In this work, we focus on the position-space procedure [1, 2], in which the renormalization condition for an operator is imposed on the corresponding correlation function in position space. It is an important advantage of this procedure that it provides a fully gauge invariant renormalization prescription since the correlator used in the renormalization condition is gauge invariant. This advantage prevents the mixing with gauge noninvariant operators that occurs in gauge noninvariant schemes such as the regularization independent momentum subtraction (RI/MOM) scheme [3]. Since the operators appearing in the position-space renormalization prescription are evaluated at separated space-time points, operators which vanish when the equations of motion are imposed will also not contribute. Therefore a position-space renormalization scheme will also avoid mixing with operators which vanish by the equations of motion – mixing which can occur in the RI/MOM approach.

An important difficulty of the position-space approach arises from the discrete lattice of points on which the position space Green's function is evaluated. Unless one works with lattices whose lattices spacings are related as integer multiples, errors may be introduced when combining results from two different ensembles. Combining results from ensembles with different lattice spacing is necessary both when evaluating the continuum limit and when using step scaling [4–6]. (For example, when Cichy *et al.* [7] employ step scaling in position space they consider lattice spacings which differ by factors of two.) Recall that step scaling is an important nonperturbative method used to relate the normalization of operators that are being used in a coarse lattice calculation to physically equivalent operators defined on a fine, weak-coupling lattice where a connection to perturbatively normalized operators can be more accurately made.

In an RI/MOM scheme the Fourier transform averages over the discrete lattice and the resulting functions of momentum approach their continuum limits in a well-understood fashion [8, 9]. In this paper we propose an alternative average that partially smooths the

discrete nature of the position-space lattice while working with gauge invariant quantities and maintaining a non-zero separation between the operators whose Green's functions are being studied.

Our strategy is best illustrated using two-point functions, which are the starting point of the present position-space renormalization schemes, as illustrated by the expression

$$G(x_n) = \langle \mathcal{O}(x_n) \mathcal{O}(0)^\dagger \rangle \quad (1)$$

where \mathcal{O} is a gauge-invariant composite local operator, x_n is a point on our discrete lattice determined by the four integers $n = (n_1, n_2, n_3, n_4)$ and, for simplicity, the second point 0 is chosen to be the origin, also a point of this lattice. As is described in more detail in Section III, we begin by extending this function into a function $\overline{G}(x)$ of the continuous position four-vector x , obtained by multi-linear interpolation from the sixteen values obtained by evaluating $G(x_n)$ at the sixteen lattice points that lie at the vertices of the four-dimensional cube which contains the point x .

Assuming, as we do throughout this paper, that our lattice theory has no order a errors, our interpolated Green's function $\overline{G}(x)$ will agree with the corresponding Green's function of the continuum theory up to errors which vanish as a^2 in the continuum limit. Of course, the a^2 errors which appear in the piece-wise linear function $\overline{G}(x)$ will still reflect the $O(4)$ symmetry breaking of the underlying lattice. In order to reduce these lattice artifacts and define a function of a single scale, we further simplify our Green's function by averaging the point x over a three-dimension sphere of radius $|x|$ centered at the origin:

$$\widehat{G}(|x|) = \frac{1}{2\pi^2|x|^3} \int d^4x' \delta(|x'| - |x|) \overline{G}(x'). \quad (2)$$

We will then impose conditions on $\widehat{G}(|x|)$ to renormalize the operator \mathcal{O} .

The finite lattice spacing errors that are present in the lattice Green's function $G(x_n)$ are expected to appear as simple polynomials in a with coefficients which in perturbation theory depend only logarithmically in a , allowing a simple extrapolation to the continuum limit. The lattice spacing dependence of our averaged quantity $\widehat{G}(|x|)$ will be more complicated. In addition to the simple a^2 errors coming from $G(x_n)$, the sphere averaging procedure will introduce $O(a^2)$ errors which, while bounded by a^2 may be complicated irregular functions of a which could cause an explicit extrapolation in a^2 to fail. As will be shown in Appendix A, this irregular dependence on a appears to be negligible, making the scheme proposed here

suitable for a calculation in which the continuum limit is to be evaluated. Of course, were this error too large, we may be able to introduce a higher-order interpolation scheme which would make these troubling effects of higher order than a^2 and therefore systematically negligible.

As an example of the spherical average, we present our result for the quark mass renormalization, which can be done by renormalizing the scalar current. There are several previous works on position-space renormalization of bilinear operators [2, 10, 11]. For renormalization of bilinear operators, there is another important advantage of the position-space procedure: the perturbative matching to the modified minimal subtraction ($\overline{\text{MS}}$) scheme is available to $O(\alpha_s^4)$ for the vector, axial-vector, scalar and pseudoscalar currents and to $O(\alpha_s^3)$ for the tensor current [12]. Utilizing the spherical averaging technique, we perform a new analysis that takes the continuum limit of the renormalized quark mass at many values of $|x|$ and shows its $|x|$ -dependence. The final result agrees with the FLAG average [13] as well as our previous result using the RI/SMOM scheme [14, 15], an improved version of the RI/MOM scheme with reduced sensitivity to long-distance effects, for the same ensembles [16].

An important future use for this sphere-averaged position-space renormalization scheme is to accurately define the weak operators which are needed in the calculation of non-leptonic decays, such as the $K \rightarrow \pi\pi$ decay, in a three-flavor theory. At present these three-flavor operators are determined by using QCD perturbation theory to calculate that combination of three-flavor operators which will give the same matrix elements as the more physical four-flavor operators when evaluated at energies below the charm threshold. Such a use of QCD perturbation theory below the charm threshold introduces uncontrolled systematic errors. However, a nonperturbative matching of three- and four-flavor operators using RI/MOM methods is also potentially uncertain. The gauge-noninvariant operators that are traditionally neglected in RI/MOM calculations when performed at higher energies because of the presence of explicit factors of the gluon field, may give large contributions at energies below the charm mass. The sphere-averaged position-space renormalization scheme may allow a nonperturbative determination of the three-flavor Wilson coefficients in which the only errors, which are systematically improvable, come from the neglect of higher-dimension operators proportional to inverse powers of the charm quark mass.

The paper is organized as follows. In Section II, we summarize the traditional procedure of the position-space renormalization of an operator that does not mix with any other

operator and identify the problem posed by the discretization errors that is addressed by the method presented in this paper. Our core technique in this work, the spherical average, is introduced in Section III. In Section IV, a concrete strategy to calculate the renormalized quark mass through the position-space renormalization of the scalar current is proposed. In Section V, the details of the numerical simulation is described. In Section VI, our final result for the renormalized quark mass is shown. In the process, we show the performance of the spherical average especially at short distances and discuss how the renormalization window can be extended. In addition, we present a test of an *ad hoc* prescription to reduce nonperturbative effects at long distances that are mainly due to instanton interactions. In Section VII, we summarize the paper and discuss the prospect of further applications of the spherical average for various quantities calculated on the lattice. In Appendix A, we describe our investigation of the irregular a -dependence that appears in the spherical average, which turns out to be negligible.

II. FUNDAMENTAL PROCEDURE IN PREVIOUS WORKS

In this section, we summarize the traditional approach to position-space renormalization of an operator that does not mix with any other operator. We consider two-point Green's functions of a composite operator $\mathcal{O}^s(\mu; x)$ renormalized at a scale μ in a scheme s and the corresponding lattice operator $\mathcal{O}^{\text{lat}}(1/a; an)$ for a lattice spacing a ,

$$G_{\mathcal{O}}^s(\mu; x) = \langle \mathcal{O}^s(\mu; x) \mathcal{O}^s(\mu; 0)^\dagger \rangle, \quad G_{\mathcal{O}}^{\text{lat}}(1/a; an) = \langle \mathcal{O}^{\text{lat}}(1/a; an) \mathcal{O}^{\text{lat}}(1/a; 0)^\dagger \rangle. \quad (3)$$

Here, we distinguish a four-dimensional point in the continuum theory $x = (x_1, x_2, x_3, x_4)$ from that on the lattice $an = (an_1, an_2, an_3, an_4)$ since the discrete character of the lattice points is carefully considered throughout the paper. In this section, we treat these two-point functions in the chiral limit, which does not require consideration of the mass renormalization of quarks in the correlators and remove an extra scale from the renormalization procedure.

An operator $\mathcal{O}^X(\mu; x)$ renormalized at μ in the X-space scheme [2, 10] is defined in the continuum theory by the condition

$$G_{\mathcal{O}}^X(\mu; x) \Big|_{\mu=1/|x|} = G_{\mathcal{O}}^{\text{free}}(x), \quad (4)$$

where $G_{\mathcal{O}}^{\text{free}}(x)$ is the corresponding two-point Green's function evaluated in free field theory and $|x| = \sqrt{\sum_{\mu} x_{\mu}^2}$. Since this nonperturbative scheme is fully gauge invariant and free from

contact terms unlike the RI/MOM scheme, it prevents mixing with irrelevant operators and thus is a quite convenient scheme especially at low energies where perturbative schemes are not applicable and mixing with many irrelevant operators can occur in gauge noninvariant schemes.

The traditional renormalization condition

$$\tilde{Z}_{\mathcal{O}}^{X/\text{lat}}(\mu, 1/a; an)^2 \Big|_{\mu=1/a|n|} G_{\mathcal{O}}^{\text{lat}}(1/a; an) = G_{\mathcal{O}}^{\text{free}}(x) \Big|_{x=an}, \quad (5)$$

yields

$$\tilde{Z}_{\mathcal{O}}^{X/\text{lat}}(\mu, 1/a; an) \Big|_{\mu=1/a|n|} = \sqrt{\frac{G_{\mathcal{O}}^{\text{free}}(x) \Big|_{x=an}}{G_{\mathcal{O}}^{\text{lat}}(1/a; an)}}, \quad (6)$$

which violates rotational symmetry and depends on n in a complicated way. Since the $O(4)$ -violating n -dependence is $O(a^2)$, it can be eliminated and only the dependence on the distance scale $\mu = 1/a|n|$ remains if the continuum limit of the renormalized operator $\tilde{Z}_{\mathcal{O}}^{X/\text{lat}}(\mu, 1/a; an) \mathcal{O}^{\text{lat}}(1/a; an')$ is accurately taken. However, evaluating the continuum limit requires an a^2 extrapolation of numerical values at a fixed physical location $x = a_A n_A = a_B n_B = \dots$ so that when comparing ensembles A and B it is only the lattice spacing, not the physical position which is changing. This means the ratios of the lattice spacings for the ensembles used to evaluate the continuum limit need to be integers or simple rational numbers. However, lattice spacings are not tuned so precisely in practical simulations. We propose a way to circumvent this problem in the next section.

We close the section by describing the relation between operators in the X -space scheme and those in another scheme s . Using Eqs. (3) and (4), the matching factor $Z_{\mathcal{O}}^{s/X}(\mu, \mu')$, which is defined by $\mathcal{O}^s(\mu; x) = Z_{\mathcal{O}}^{s/X}(\mu, \mu') \mathcal{O}^X(\mu'; x)$, can be written as

$$Z_{\mathcal{O}}^{s/X}(\mu, \mu') = \sqrt{\frac{G_{\mathcal{O}}^s(\mu; x)}{G_{\mathcal{O}}^{\text{free}}(x)}} \Big|_{|x|=1/\mu'}. \quad (7)$$

If we already know the correlator in the scheme s and any treatments in the X -space scheme such as the step scaling are not needed, we can skip renormalizing operators to the X -space scheme and directly compute

$$\tilde{Z}_{\mathcal{O}}^{s/\text{lat}}(\mu, 1/a; an) \equiv Z_{\mathcal{O}}^{s/X}(\mu, \mu') \tilde{Z}_{\mathcal{O}}^{X/\text{lat}}(\mu', 1/a; an) \Big|_{\mu'=1/a|n|} = \sqrt{\frac{G_{\mathcal{O}}^s(\mu; x) \Big|_{x=an}}{G_{\mathcal{O}}^{\text{lat}}(1/a; an)}}. \quad (8)$$

Of course, this expression violates rotational symmetry as does Eq. (6) and therefore suffers from the same difficulty in taking the continuum limit of the corresponding renormalized operator as is described above.

III. SMOOTHING AVERAGE OVER SPHERES

Renormalization factors determined through the procedure discussed in the previous section contain discretization errors which depend in a complicated way on the lattice point n where the renormalization condition is imposed due to the violation of rotational symmetry. The complicated discretization errors induce difficulty in taking the continuum limit of renormalized operators as mentioned in the previous section. Some ideas to reduce this kind of discretization errors, subtracting free-field discretization error [2, 11] and discarding the lattice data points where discretization errors are quite large [10, 17], have been applied. These previous works usually naïvely averaged the renormalization factor Eq. (8) over lattice points in the renormalization window, which could induce an irrelevant linear dependence on a and further degrade the accuracy of the continuum extrapolation of a renormalized quantity which assumed that the leading discretization error is $O(a^2)$. In this section, we propose another way to smooth lattice results, in which the irrelevant $O(a^1)$ discretization error does not appear and the continuum extrapolation of a renormalized quantity using a constant plus an $O(a^2)$ term can be safely taken.

We consider a lattice quantity $f_{a,n}$ calculated at each lattice point n . The a -dependence of $f_{a,n}$ can be sketched as

$$f_{a,n} = F(x; a)|_{x=an} + c_{a,n}a^2 + O(a^4), \quad (9)$$

with a coefficient $c_{a,n}$ which depends on the lattice point n in a complicated way. In the simplest case, $F(x; a)$ is the continuum limit of the quantity being computed and does not depend on a . However, by including a possible logarithmic a -dependence, we can make our discussion more general and include the case where $f_{a,n}$ is an n -dependent renormalization factor such as the quantities given in Eqs. (6) and (8) or a correlator of unrenormalized operators.

We start with the case of one dimension, where we assume $x = x_1$. We then use linear interpolation to extend the lattice results for $f_{a,n}$, to define a function $\bar{f}_a(x)$ for all values of the continuous physical distance x :

$$\bar{f}_a(x) = \frac{(a(n+1) - x)f_{a,n} + (x - an)f_{a,n+1}}{a}, \quad (10)$$

where n is now defined as $\lfloor x/a \rfloor$, the largest integer that is less than or equal to x/a . Inserting Eq. (9) into this equation and expanding $F(an; a)$ and $F(a(n+1); a)$ around x , we

see that $\bar{f}_a(x)$ is an approximation to $F(x; a)$ as a continuous function of x that is accurate up to $O(a^2)$. Note that the appropriate weight of $a(n+1) - x$ and $x - an$ in Eq. (10) is important to avoid introducing an $O(a^1)$ error which would spoil the accuracy of an a^2 continuum extrapolation.

In the case of two dimensions, the weighted average Eq. (10) can be modified to a bilinear interpolation

$$\bar{f}_a(x) = a^{-2} \begin{pmatrix} a(n_1+1) - x_1 & x_1 - an_1 \end{pmatrix} \begin{pmatrix} f_{a,n} & f_{a,n+\hat{2}} \\ f_{a,n+\hat{1}} & f_{a,n+\hat{1}+\hat{2}} \end{pmatrix} \begin{pmatrix} a(n_2+1) - x_2 \\ x_2 - an_2 \end{pmatrix}, \quad (11)$$

where $n_\mu = \lfloor x_\mu/a \rfloor$ and $\hat{\mu}$ is the unit vector for the μ -direction. While this weighted average is also easily found to be free from the $O(a^1)$ error, it is expected to depend significantly on the direction of x as well as the distance $|x|$ due to the violation of rotational symmetry. The most naïve way to smooth this discretization error may be to introduce the average over a circle with the radius of $|x|$,

$$\hat{f}_a(|x|) = \frac{1}{2\pi} \int_0^{2\pi} d\theta \bar{f}_a(x), \quad (12)$$

where we use two-dimensional polar coordinates

$$x_1 = |x| \cos \theta, \quad x_2 = |x| \sin \theta. \quad (13)$$

The extension to four dimensions is straightforward. The interpolation of f_a at x is given by

$$\bar{f}_a(x) = a^{-4} \sum_{i,j,k,l=0}^1 \Delta_{1,i} \Delta_{2,j} \Delta_{3,k} \Delta_{4,l} f_{a,n+i\hat{1}+j\hat{2}+k\hat{3}+l\hat{4}}, \quad (14)$$

where we define the factors

$$\Delta_{\mu,i} = |a(n_\mu + 1 - i) - x_\mu|. \quad (15)$$

One can easily verify this interpolated value is also free from the $O(a^1)$ error. The smoothing average over the four-dimensional sphere with the radius of $|x|$ is

$$\hat{f}_a(|x|) = \frac{1}{2\pi^2} \int_0^\pi d\theta_1 \int_0^\pi d\theta_2 \int_0^{2\pi} d\theta_3 \sin^2 \theta_1 \sin \theta_2 \bar{f}_a(x), \quad (16)$$

with four-dimensional polar coordinates

$$\begin{aligned}
x_1 &= |x| \cos \theta_1, \\
x_2 &= |x| \sin \theta_1 \cos \theta_2, \\
x_3 &= |x| \sin \theta_1 \sin \theta_2 \cos \theta_3, \\
x_4 &= |x| \sin \theta_1 \sin \theta_2 \sin \theta_3.
\end{aligned} \tag{17}$$

The averaged quantity $\hat{f}_a(|x|)$ will differ from the direction independent continuum quantity $F(x; a)$ by discretization errors of $O(a^2)$.

Although the discretization error of the spherical average is thus $O(a^2)$, it should be noted that the averaged value is not a regular polynomial in a but will contain extra non-differentiable terms of $O(a^2)$ because of the complicated a -dependence of the floor function $n_\mu = \lfloor x_\mu/a \rfloor$. This irregularity could arise also from the fact that the set of the lattice points n and their weight used by the spherical average at each fixed physical distance $|x|$ depend on the lattice spacing a . Such complicated a -dependence could spoil the accuracy of a continuum extrapolation which assumed a regular a^2 term. In Appendix A, we discuss the significance of such complicated a -dependence and demonstrate it is small.

IV. QUARK MASSES RENORMALIZATION IN POSITION SPACE

A. Strategy

Since the quark mass renormalization factor Z_m can be calculated as the inverse of the renormalization factor Z_S of the scalar current $S(x) = \bar{u}(x)d(x)$, we consider the renormalization of $S(x)$, which is equivalent to that of the pseudoscalar current $P(x) = \bar{u}(x)i\gamma_5 d(x)$ as long as chiral symmetry on the lattice is maintained. Since we use domain-wall fermions, we can calculate Z_m from the renormalization of $S(x)$ and $P(x)$.

In what follows, we employ the $\overline{\text{MS}}$ scheme and introduce the input light quark mass parameter m'_{ud} that is used for the calculation of the correlators on the lattice. The n -dependent renormalization factor Eq. (8) is then rewritten as

$$\tilde{Z}_{S/P}^{\overline{\text{MS}}/\text{lat}}(\mu, 1/a; an; m'_{ud}) = \sqrt{\frac{G_S^{\overline{\text{MS}}}(\mu; x; 0)|_{x=an}}{G_{S/P}^{\text{lat}}(1/a; an; m'_{ud})}}. \tag{18}$$

The chiral limit ($m'_{ud} \rightarrow 0$) is taken in Section VI. In this work, the scalar correlator $G_S^{\overline{\text{MS}}}$ in continuum perturbation theory is considered only in the massless limit, where it is equivalent to the pseudoscalar correlator and is available to $O((\alpha_s/\pi)^4)$ accuracy [12]. The strategy to improve the convergence of the perturbative series of the correlator is discussed in the following subsection and in [11] for more detail.

We also analyze an $O(4)$ -symmetric renormalization factor

$$\widehat{\widetilde{Z}}_{S/P}^{\overline{\text{MS}}/\text{lat}}(\mu, 1/a; |x|; m'_{ud}) = Z_S^{\overline{\text{MS}}/X}(\mu, \mu') \widehat{\widetilde{Z}}_{S/P}^{X/\text{lat}}(\mu', 1/a; |x|; m'_{ud}) \quad (19)$$

obtained from Eq. (7) and the $O(4)$ -symmetric renormalization condition

$$\widehat{\widetilde{Z}}_{S/P}^{X/\text{lat}}(\mu, 1/a; |x|; m'_{ud})^2 \Big|_{\mu=1/|x|} \widehat{G}_{S/P}^{\text{lat}}(1/a; |x|) = G_S^{\text{free}}(x), \quad (20)$$

with the sphere-averaged Green's function $\widehat{G}_S^{\text{lat}}(1/a; |x|)$ calculated as follows. It should be noted that the complicated a -dependence appearing in the multi-linear interpolation depends on the first and second derivatives of the continuum version of the function that is to be interpolated with respect to $|x|$. Therefore, the spherical averaging procedure is applied to a function whose $|x|$ -dependence in the continuum limit is as small as possible. For this reason, we calculate the spherical average of the ratio $G_{S/P}^{\text{lat}}(1/a; an; m'_{ud})/G_S^{\text{free}}(x)|_{x=an}$ at each distance $|x|$ and then define the sphere-averaged Green's function $\widehat{G}_S^{\text{lat}}(1/a; |x|)$ as the product of it and $G_S^{\text{free}}(x)$.

Note that either $\widehat{\widetilde{Z}}_{S/P}^{\overline{\text{MS}}/\text{lat}}(\mu, 1/a; an; m'_{ud})$ or $\widehat{\widetilde{Z}}_{S/P}^{\overline{\text{MS}}/\text{lat}}(\mu, 1/a; |x|; m'_{ud})$ may not be an appropriate renormalization factor since it still depends on the location n or $|x|$ due to the following sources of error:

- Discretization effects in $G_{S/P}^{\text{lat}}(1/a; an; m'_{ud})$.
- Truncation error from the perturbative calculation of $G_S^{\overline{\text{MS}}}(\mu; x; 0)$.
- Nonperturbative QCD effects, which are not present in the perturbatively calculated $G_S^{\overline{\text{MS}}}(\mu; x; 0)$ but do appear in the nonperturbatively measured $G_{S/P}^{\text{lat}}(1/a; an; m'_{ud})$.

The first source is uncontrollable at short distances ($|x|, a|n| \sim a$), while the others are significant at long distances ($|x|, a|n| \gtrsim 1/\Lambda_{\text{QCD}}$). We need to find or create an appropriate window where all of these sources of error are under control and the n -dependence of $\widehat{\widetilde{Z}}_{S/P}^{\overline{\text{MS}}/\text{lat}}(\mu, 1/a; an; m'_{ud})$ or $|x|$ -dependence of $\widehat{\widetilde{Z}}_{S/P}^{\overline{\text{MS}}/\text{lat}}(\mu, 1/a; |x|; m'_{ud})$ is sufficiently small.

Since the third source especially violates the degeneracy of $\tilde{Z}_S^{\overline{\text{MS}}/\text{lat}}(\mu, 1/a; an; m'_{ud})$ and $\tilde{Z}_P^{\overline{\text{MS}}/\text{lat}}(\mu, 1/a; an; m'_{ud})$, analyzing both of these may specify the region where nonperturbative effects are less significant.

Using the unrenormalized quark mass $m_q^{\text{bare}}(1/a)$ at the physical pion mass, which is given in Ref. [16] for the degenerate up and down quarks ($q = ud$) and the strange quark ($q = s$) on our ensembles, we analyze the n - and $|x|$ -dependent renormalized quark masses

$$\tilde{m}_{q,S/P}^{\overline{\text{MS}}}(\mu; an; a, m'_{ud}) = \frac{m_q^{\text{bare}}(1/a)}{\tilde{Z}_{S/P}^{\overline{\text{MS}}/\text{lat}}(\mu, 1/a; an; m'_{ud})}, \quad (21)$$

and

$$\hat{\tilde{m}}_{q,S/P}^{\overline{\text{MS}}}(\mu; |x|; a, m'_{ud}) = \frac{m_q^{\text{bare}}(1/a)}{\hat{\tilde{Z}}_{S/P}^{\overline{\text{MS}}/\text{lat}}(\mu, 1/a; |x|; m'_{ud})}, \quad (22)$$

where $q = ud, s$.

In Section VI, we determine the renormalized mass of the degenerate up and down quarks and the strange quark on our ensembles.

B. Scalar correlator in massless perturbation theory

While the available four-loop perturbative results is an important advantage of the position-space renormalization of the scalar current, the region where discretization errors may be under controlled is $1/|x| \lesssim 1$ GeV for currently available lattices with domain-wall fermions and therefore the convergence of the perturbative expansion might be still insufficient. The convergence can be improved by a resummation of the perturbative series using the coupling constant at another renormalization scale as explained below.

Chetyrkin and Maier [12] gave the coefficients $C_i^{S,\text{CM}}$ of the perturbative expansion

$$G_S^{\overline{\text{MS}}}(\tilde{\mu}_x; x; 0) = \frac{3}{\pi^4 |x|^6} \left(1 + \sum_i C_i^{S,\text{CM}} a_s(\tilde{\mu}_x)^i \right), \quad (23)$$

up to $i = 4$. Here, the strong coupling constant $a_s(\tilde{\mu}_x) = \alpha_s(\tilde{\mu}_x)/\pi$ is renormalized in the $\overline{\text{MS}}$ scheme at $\tilde{\mu}_x = 2e^{-\gamma_E}/|x| \simeq 1.123/|x|$ with Euler's constant $\gamma_E = 0.5772$ and is evaluated using the scale of QCD $\Lambda_{\text{QCD}}^{\overline{\text{MS}}} = 332(17)$ [18] in three flavor theory. By setting the renormalization scale $\tilde{\mu}_x$ of the scalar current and the strong coupling constant proportional to $|x|^{-1}$, the logarithmic $|x|$ -dependence of the perturbative coefficients can be eliminated.

The anomalous dimension of the scalar current, which is the same as the mass anomalous dimension except for the sign and is calculated up to the five-loop level [19], enables us to evolve the scale on the LHS of Eq. (23). The beta function, which is also available to the five-loop level [20], can be used to evolve the scale of the strong coupling constant on the RHS of Eq. (23). Using the original perturbative coefficients $C_i^{S,\text{CM}}$ and these scale evolution procedures, we obtain a general expression of the perturbative series

$$G_S^{\overline{\text{MS}}}(\mu'_x; x; 0) = \frac{3}{\pi^4 x^6} \left(1 + \sum_i C_i^S(\mu_x^*, \mu'_x) a_s(\mu_x^*)^i \right), \quad (24)$$

where μ'_x and μ_x^* are the renormalization scale of the scalar current and that of the strong coupling constant, respectively. While the all-order calculation of the RHS is supposed to be independent of μ_x^* , any finite-order calculation does depend on μ_x^* . Therefore, the convergence of the perturbative series can be investigated by varying μ_x^* .

Thus, we obtain the numerical value of the scalar correlator $G_S^{\overline{\text{MS}}}(\mu'_x; x; 0)|_{\mu_x^*}$ calculated with a scale μ_x^* of the strong coupling constant. In order to renormalize the scalar current at a specific scale, which we set to 3 GeV, the scale evolution is needed from μ'_x to 3 GeV,

$$\begin{aligned} G_S^{\overline{\text{MS}}}(3 \text{ GeV}; x; 0)|_{\mu_x^*, \mu'_x} &= \exp \left(-2 \int_{a_s(\mu'_x)}^{a_s(3 \text{ GeV})} \frac{dz}{z} \frac{\gamma_m(z)}{\beta(z)} \right) G_S^{\overline{\text{MS}}}(\mu'_x; x; 0)|_{\mu_x^*} \\ &= \left(\frac{\rho(a_s(\mu'_x))}{\rho(a_s(3 \text{ GeV}))} \right)^2 G_S^{\overline{\text{MS}}}(\mu'_x; x; 0)|_{\mu_x^*}, \end{aligned} \quad (25)$$

where $\gamma_m(z)$ and $\beta(z)$ are the mass anomalous dimension and the beta function, respectively, and $\rho(z)$ is known to the five-loop level [19]. While $G_S^{\overline{\text{MS}}}(3 \text{ GeV}; x; 0)|_{\mu_x^*, \mu'_x}$ is also supposed to be independent of μ_x^* and μ'_x in an all-order calculation, the convergence can be optimized by tuning the scale parameters μ'_x and μ_x^* so that the dependence on these scale parameters is minimized. We use the optimal values $\mu'_x = e^{0.8}/|x| \simeq 2.2/|x|$ and $\mu_x^* = e^{1.05}/|x| \simeq 2.9/|x|$ in the case of three-flavor QCD quoted by Ref. [11].

V. LATTICE SETUP

We perform lattice simulation with the ensembles of 2 + 1-flavor dynamical domain-wall fermions [21, 22] and the Iwasaki gauge action [23, 24] generated by the RBC and UKQCD collaborations [16]. Table I summarizes the properties of the ensembles used in this work. We calculate with three lattice cutoffs ranging from 1.785(5) GeV to 3.148(17) GeV. The

TABLE I. Lattice ensembles used in this work.

Ensemble set	β	a^{-1} [GeV]	$L^3 \times T \times L_s$	am'_s	am'_{ud}	aM_π	N_{conf}
24I	2.13	1.785(5)	$24^3 \times 64 \times 16$	0.0400	0.0050	0.1904(6)	137
					0.0100	0.2422(5)	77
32I	2.25	2.383(9)	$32^3 \times 64 \times 16$	0.0300	0.0040	0.1269(4)	157
					0.0080	0.1727(4)	110
32Ifine	2.37	3.148(17)	$32^3 \times 64 \times 12$	0.0186	0.0047	0.1179(13)	170

 TABLE II. Values of $Z_q(1/a)$ quoted from Ref. [16].

Ensemble set	Z_{ud}	Z_s
24I	0.9715(54)	0.9628(40)
32I	1	1
32Ifine	1.015(17)	1.005(12)

coarsest ensembles (24I) and the finer ones (32I and 32Ifine) are generated on the $24^3 \times 64$ and $32^3 \times 64$ lattices, respectively. The strange quark mass m'_s is used only for the strange sea quark, while we use the same values of the sea and valence quark masses m'_{ud} for the degenerate up and down quarks. The corresponding pion masses of the ensembles are quoted from Refs. [16, 25] and in the region from 300 MeV to 430 MeV.

We distinguish the input quark masses m'_q ($q = ud, s$), which are used in the lattice calculations and shown in Table I, from the renormalized and unrenormalized quark masses ($m_q^{\overline{\text{MS}}}(\mu)$ and $m_q^{\text{bare}}(1/a)$) that realize the physical pion mass. In Ref. [16], the values of unrenormalized quark masses were represented by

$$m_q^{\text{bare}}(1/a) = \frac{m_q^{\text{bare}, 32\text{I}}}{Z_q(1/a)}, \quad (26)$$

where the values of quantities on the RHS were obtained by a global continuum and chiral fit to ten ensembles in the continuum scaling with the input experimental values of pion, kaon and Omega baryon masses [16]. We use $m_{ud}^{\text{bare}, 32\text{I}} = 2.198(11)$ MeV, $m_{ud}^{\text{bare}, 32\text{I}} = 60.62(24)$ MeV and $Z_q(1/a)$ summarized in Table II.

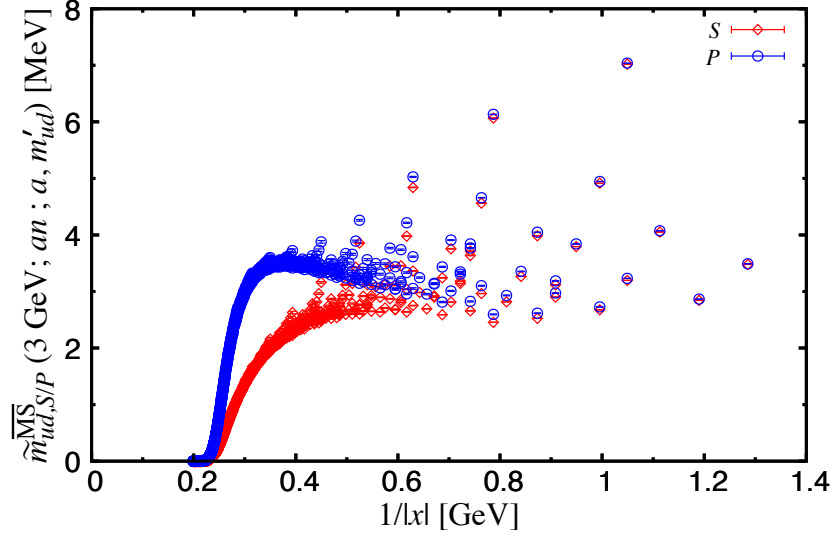


FIG. 1. Results for $\tilde{m}_{ud,S/P}^{\overline{\text{MS}}}(3 \text{ GeV}; an; a, m'_{ud})$ calculated on the 32Ifine ensemble. The perturbative calculation is done at $\mu_x^* = e^{1.05}/|x|$ and $\mu'_x = e^{0.80}/|x|$.

For each configuration, we calculate the scalar and pseudoscalar correlators with 16 point sources located at

$$\begin{aligned}
& (0, 0, 0, 0), \quad (\frac{L}{2}, \frac{L}{2}, 0, 0), \quad (0, \frac{L}{2}, \frac{L}{2}, 0), \quad (\frac{L}{2}, 0, \frac{L}{2}, 0), \\
& (\frac{L}{4}, \frac{L}{4}, \frac{L}{4}, \frac{T}{4}), \quad (\frac{3L}{4}, \frac{3L}{4}, \frac{L}{4}, \frac{T}{4}), \quad (\frac{L}{4}, \frac{3L}{4}, \frac{3L}{4}, \frac{T}{4}), \quad (\frac{3L}{4}, \frac{L}{4}, \frac{3L}{4}, \frac{T}{4}), \\
& (\frac{L}{2}, \frac{L}{2}, \frac{L}{2}, \frac{T}{2}), \quad (0, 0, \frac{L}{2}, \frac{T}{2}), \quad (\frac{L}{2}, 0, 0, \frac{T}{2}), \quad (0, \frac{L}{2}, 0, \frac{T}{2}), \\
& (\frac{3L}{4}, \frac{3L}{4}, \frac{3L}{4}, \frac{3T}{4}), \quad (\frac{L}{4}, \frac{L}{4}, \frac{3L}{4}, \frac{3T}{4}), \quad (\frac{3L}{4}, \frac{L}{4}, \frac{L}{4}, \frac{3T}{4}), \quad (\frac{L}{4}, \frac{3L}{4}, \frac{L}{4}, \frac{3T}{4}),
\end{aligned} \tag{27}$$

and average the correlators over all these source points.

VI. NUMERICAL RESULTS

Figure 1 shows $\tilde{m}_{ud,S/P}^{\overline{\text{MS}}}(3 \text{ GeV}; x; a, m'_{ud})$ defined in Eq. (21) calculated on the 32Ifine ensemble. The results for both the scalar (diamonds) and pseudoscalar (circles) channels are shown. Because of the violation of rotational symmetry, we distinguish, in the figure, different lattice points that are not equivalent with respect to 90° rotations or parity inversion in the four-dimensional hypercubic group. For example, $(1,1,1,1)$ and $(2,0,0,0)$ correspond to the same distance $a|n|$ but are distinguished since they are indeed different points if rotational symmetry is violated and only hypercubic symmetry remains. The results are averaged over sets of lattice points related by 90° rotations including parity inversion.

The n -dependence of this quantity arises mainly from discretization errors at short distances, the truncation error of the perturbative calculation and nonperturbative effects at long distances as explained in Section IV A. These sources of the n -dependence need to be under controlled in order to obtain the correct value of the renormalized mass $m_q^{\overline{\text{MS}}}(3 \text{ GeV})$. However, Figure 1 indicates the ambiguity due to such n -dependence is $O(1 \text{ MeV})$, which is much larger than the uncertainty of the renormalized light quark mass calculated by other works.

A rapid decrease is seen below $1/|x| = 1/a|n| \sim 0.3 \text{ GeV}$ since the truncation uncertainty of the perturbative calculation increases tremendously below this threshold. We do not expect that this lower limit on the perturbative window can be decreased because the convergence is already optimized by our choice of $\mu_x^* = e^{1.05}/|x|$ and $\mu'_x = e^{0.80}/|x|$. These choices are found to maintain reasonable convergence down to $1/|x| \sim 0.4 \text{ GeV}$ [11].

Among the three sources of n -dependence listed in Section IV A, the n -dependence associated with the convergence of the perturbative calculation is thus already taken into account as much as possible. We discuss and take into account the remaining two sources below. The n -dependence associated with discretization errors can be reduced by the spherical average designed in Section III. The third source of n -dependence associated with nonperturbative effects can be investigated by comparing the scalar and pseudoscalar channels. While Figure 1 provides some information, we prefer to take the spherical average first and then to discuss the difference between the scalar and pseudoscalar correlators.

Figure 2 shows the result for $\widehat{m}_{ud,S/P}^{\overline{\text{MS}}}(3 \text{ GeV}; x; a)$ defined in Eq. (22), where the renormalization factors of the scalar (diamonds) and pseudoscalar (circles) currents are calculated using the spherical average of the corresponding Green's functions calculated on the 32I ensembles with $am'_{ud} = 0.004$ (filled points) and $am'_{ud} = 0.008$ (open points). While discretization errors appear to be much reduced and the n -dependence is made smaller, there must still be some dependence on the regularization parameter a in the form of a^2/x^2 , $a^2\Lambda_{\text{QCD}}^2$, $a^4/|x|^4$ and so on. Therefore, the continuum extrapolation should be performed at sufficiently long distances where only $O(a^2)$ discretization errors are visible. On the other hand, the difference between the scalar and pseudoscalar channels is significant, 1% at $1/|x| \simeq 1 \text{ GeV}$ and 3% at $1/|x| \simeq 0.8 \text{ GeV}$, although we use domain-wall fermions which have high degree of chiral symmetry. Therefore, the extraction of the quark mass should be done at sufficiently short distances, $1/|x| \gtrsim 1 \text{ GeV}$ in order to obtain a systematic error less

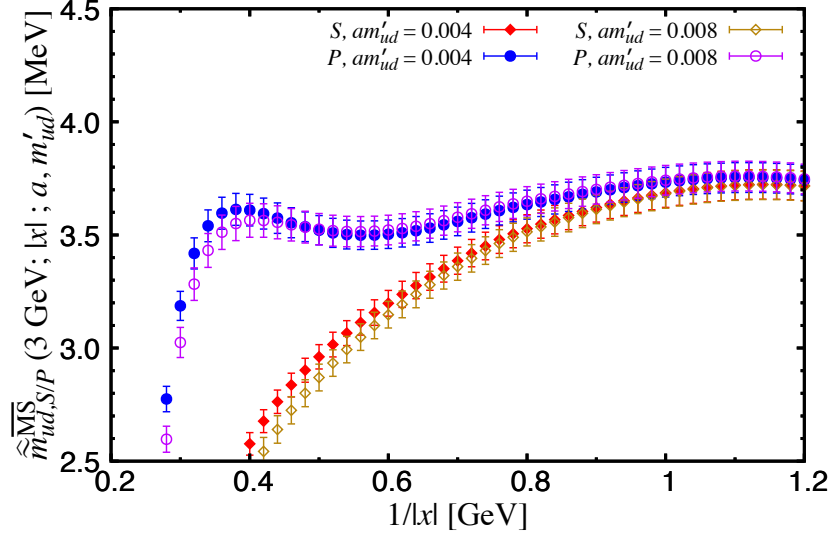


FIG. 2. Results for $\widehat{\overline{m}}_{ud,S/P}^{\overline{\text{MS}}}(3 \text{ GeV}; |x|; a, m'_{ud})$ calculated on the 32I ensembles.

than 1%. For this, the continuum extrapolation has to be safe at $1/|x| \simeq 1 \text{ GeV}$.

An important advantage of the spherical average is our ability to take the continuum limit of renormalized quantities as explained below. Since the structure of the a -dependence depends on $|x|$ as it contains a term proportional to a^2/x^2 , the renormalized quantities need to be calculated at the same physical distance scale $|x|$ for each ensemble in order to take the continuum limit as a quadratic $a^2 \rightarrow 0$ extrapolation. The spherical averaging technique trivially enables such an extrapolation. The extrapolation of the spherical average $\widehat{\overline{m}}_{ud,S/P}^{\overline{\text{MS}}}(3 \text{ GeV}; |x|; a, m'_{ud})$ to the continuum ($a \rightarrow 0$) and chiral ($m'_{ud} \rightarrow 0$) limits is done by performing a simultaneous fit to the data from all the ensembles with the fit function

$$\widehat{\overline{m}}_{ud,S/P}^{\overline{\text{MS}}}(3 \text{ GeV}; |x|; a, m'_{ud}) = \widehat{\overline{m}}_{ud,S/P}^{\overline{\text{MS}}}(3 \text{ GeV}; |x|) + C_{a,S/P}(|x|)a^2 + C_{m,S/P}(|x|)M_\pi(a, m'_{ud})^2, \quad (28)$$

with three fit parameters: $\widehat{\overline{m}}_{ud,S/P}^{\overline{\text{MS}}}(3 \text{ GeV}; |x|)$, $C_{a,S/P}(|x|)$ and $C_{m,S/P}(|x|)$ for each $|x|$. Here, we introduce a term proportional to the pion mass squared $M_\pi(a, m'_{ud})^2$ labeled by the ensemble parameters a and m'_{ud} , although the leading mass correction in perturbation theory is proportional to quark mass squared or $M_\pi(a, m'_{ud})^4$. This is because the perturbative mass correction is much smaller than the mass correction from OPE such as $m\langle\bar{q}q\rangle$ and $m\langle\bar{q}Gq\rangle$ around $1/|x| \sim 0.5 \text{ GeV}$ [17, 26].

Figure 3 shows the result for the spherical average $\widehat{\overline{m}}_{ud,S/P}^{\overline{\text{MS}}}(3 \text{ GeV}; |x|; am'_{ud})$ on each

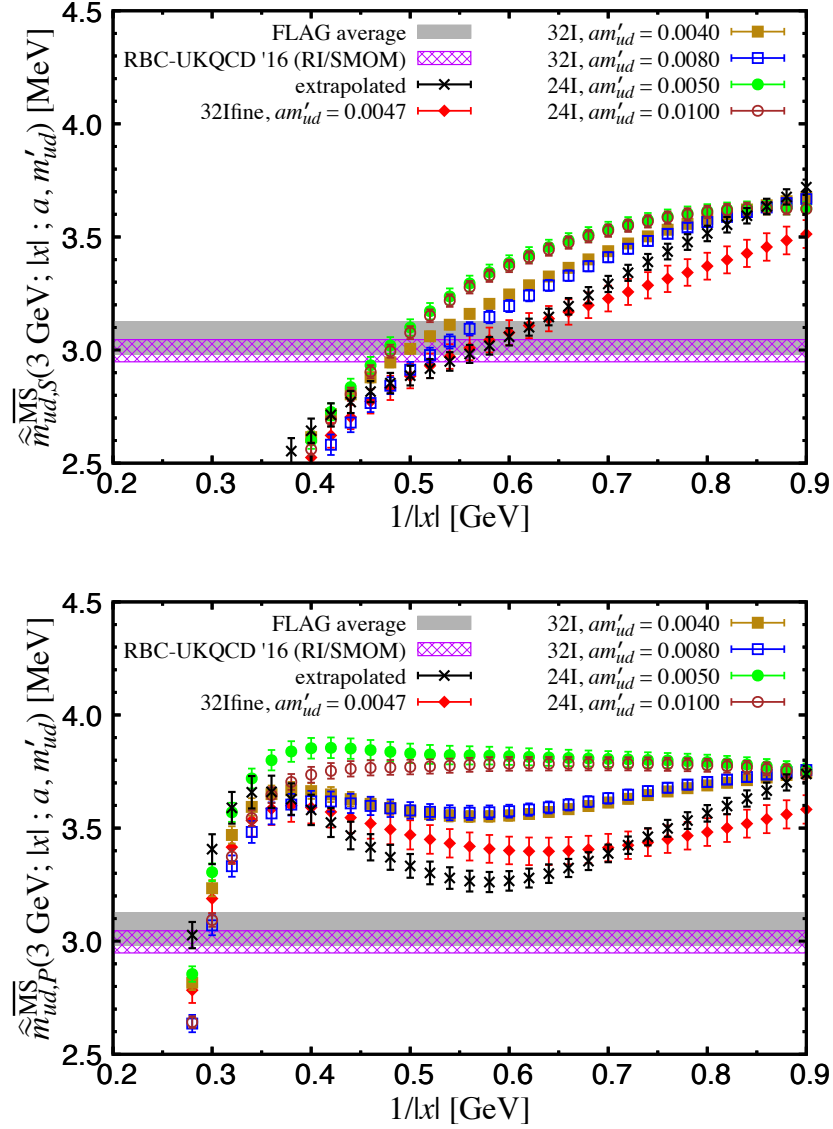


FIG. 3. Results for the spherical average $\hat{\bar{m}}_{ud,S/P}^{\overline{\text{MS}}}(3 \text{ GeV}; |x|; a, m'_{ud})$ calculated on all the ensembles listed in Table I and its extrapolation to the continuum and chiral limits ($a \rightarrow 0, m'_{ud} \rightarrow 0$). The results for the scalar (upper panel) and pseudoscalar (lower panel) channels are shown separately.

ensemble listed in Table I and its continuum and chiral limits $\hat{\bar{m}}_{ud,S/P}^{\overline{\text{MS}}}(3 \text{ GeV}; |x|)$. We also show the FLAG average [13] (solid band) and our previous RBC/UKQCD result obtained through the RI/SMOM scheme [16] (hatched band), which is $\bar{m}_{ud}^{\overline{\text{MS}}}(3 \text{ GeV}) = 2.997(49) \text{ MeV}$ including the statistical and systematic errors. While FLAG gave the value renormalized at

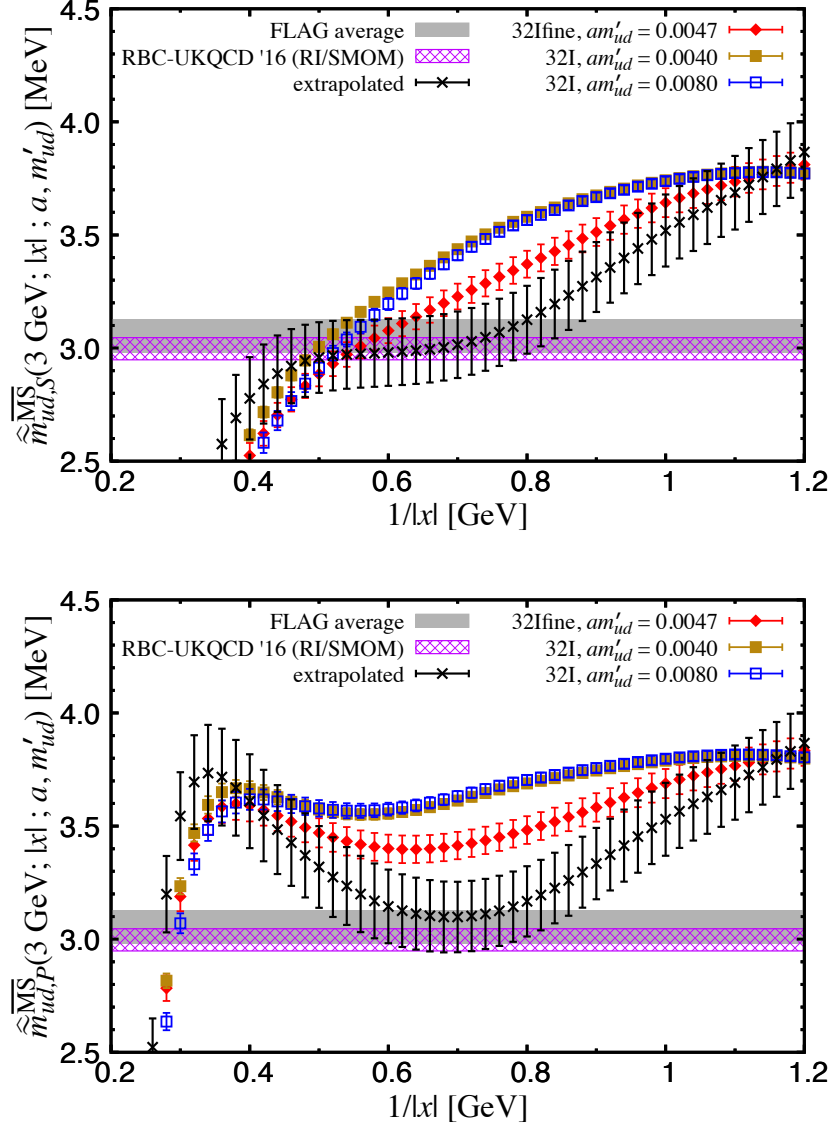


FIG. 4. Same as Figure 3 but the results only on the 32I and 32Ifine ensembles are shown and used for the extrapolation.

2 GeV [13], we perform its scale evolution to 3 GeV and show $m_{ud}^{\overline{\text{MS}}}(3 \text{ GeV}) = 3.054(72) \text{ MeV}$ in the figure. We show the result only for $1/|x| \leq 0.9 \text{ GeV}$ because the spherical average with $|x| < 2a$, which corresponds to $1/|x| > 0.89 \text{ GeV}$ on the coarsest lattice, uses the value at $x = 0$ and therefore contains unphysical contact terms. Since there is no plateau in the extrapolated results and the difference between the scalar and pseudoscalar is quite significant, it is difficult to determine the quark mass from these plots. We may need to exclude the data on the coarsest lattice from this analysis.

Figure 4 shows the results on the finer two lattices (32I and 32Ifine). The continuum limit is taken only with these lattice data, excluding the result on the coarsest ensembles. Since the number of free parameters in Eq. (28) and the number of data points in this extrapolation are both three, the extrapolation is not an actual χ^2 fit but the free parameters can still be determined, with propagated errors, by solving Eq. (28). While the $|x|$ -dependence of the extrapolated result becomes milder especially around $1/|x| \simeq 0.8$ GeV, the statistical error is substantially increased by discarding the data on the coarsest lattice. In order to obtain a reasonable result with sufficiently small statistical error from such an analysis, we need to introduce finer lattices.

Since it is currently not easy to introduce a finer lattice, we seek a more economical analysis that enables to extract the quark mass from the data we currently have. Among the three sources of the n -dependence of $\hat{Z}_{S/P}^{\overline{\text{MS}}/\text{lat}}(\mu, 1/a; an; m'_{ud})$ mentioned in Section IV A, we now focus on the third one, the nonperturbative effects. The nonperturbative effects on the scalar and pseudoscalar correlators are known to be quite large compared to those on the vector and axial-vector correlators in a model based on instantons because the scalar and pseudoscalar channels are directly affected by instantons [27, 28]. The effect of a single instanton on these channels, which is the most significant at short distances, is of the same magnitude but with opposite sign [29]. Therefore, the naïve average of these two channels may be free from the largest source of nonperturbative effects. Therefore, we analyze

$$\hat{\hat{m}}_q^{\overline{\text{MS}}} (3 \text{ GeV}; |x|; a, m'_{ud}) = \frac{m_q^{\text{bare}}(1/a)}{\hat{\hat{Z}}_{S+P}^{\overline{\text{MS}}/\text{lat}} (3 \text{ GeV}, 1/a; |x|; m'_{ud})}, \quad (29)$$

with the $O(4)$ -symmetric renormalization factor $\hat{\hat{Z}}_{S+P}^{\overline{\text{MS}}/\text{lat}} (3 \text{ GeV}, 1/a; |x|; m'_{ud})$ obtained from Eqs. (19) and (20) by substituting S/P with $S + P$ and defining $\hat{G}_{S+P}^{\text{lat}}(1/a; |x|)$ as the spherical average of the average of the scalar and pseudoscalar correlators.

Figure 5 shows the results for $\hat{\hat{m}}_{ud}^{\overline{\text{MS}}} (3 \text{ GeV}; |x|; a, m'_{ud})$. The continuum and chiral limits are taken using the fit function

$$\hat{\hat{m}}_{ud}^{\overline{\text{MS}}} (3 \text{ GeV}; |x|; a, m'_{ud}) = \hat{\hat{m}}_{ud}^{\overline{\text{MS}}} (3 \text{ GeV}; |x|) + C_a(|x|)a^2 + C_m(|x|)M_\pi(a, m'_{ud})^2, \quad (30)$$

with the fit parameters $\hat{\hat{m}}_{ud}^{\overline{\text{MS}}} (3 \text{ GeV}; |x|)$, $C_a(|x|)$ and $C_m(|x|)$. The fit results with (upper panel) and without (lower panel) the data on the coarsest lattice are shown. We see a plateau of the extrapolated data in the interval $0.4 \text{ GeV} \lesssim 1/|x| \lesssim 0.6 \text{ GeV}$ in the upper panel and

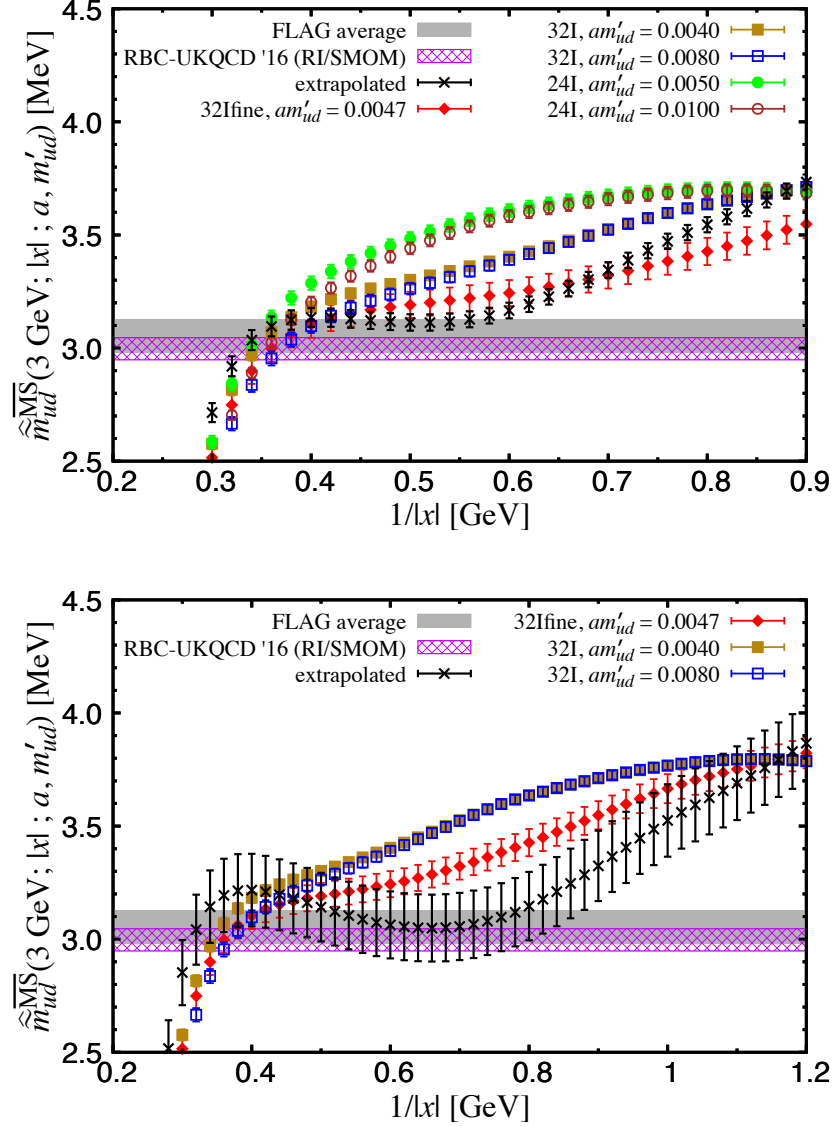


FIG. 5. Results for the spherical average $\hat{m}_{ud}^{\overline{\text{MS}}}(3 \text{ GeV}; |x|; a, m'_{ud})$ calculated from the average of the scalar and pseudoscalar correlators. The results for the extrapolation to the continuum and chiral limits ($a \rightarrow 0, m'_{ud} \rightarrow 0$) performed using all the ensembles (upper panel) and only the finer two lattices (lower panel) are also shown.

$0.4 \text{ GeV} \lesssim 1/|x| \lesssim 0.8 \text{ GeV}$ in the lower panel. These facts agree with the instanton-based observation that the nonperturbative effects on the average of the scalar and pseudoscalar correlators are much smaller than those on the individual channels.

Figure 6 shows the result for the strange quark mass defined in Eq. (29) with $q = s$, where the same renormalization factors as for the light quark mass are used. The continuum and

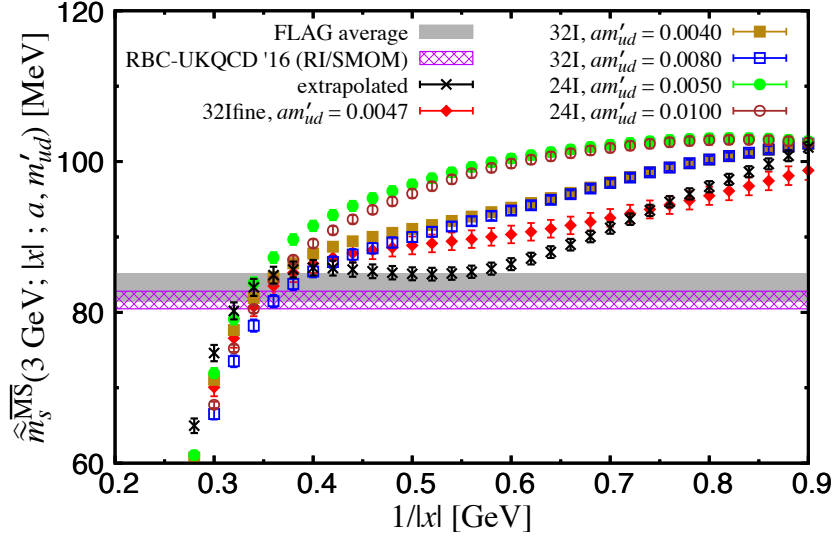


FIG. 6. Same as the upper panel of Figure 5 but the result for the strange quark mass.

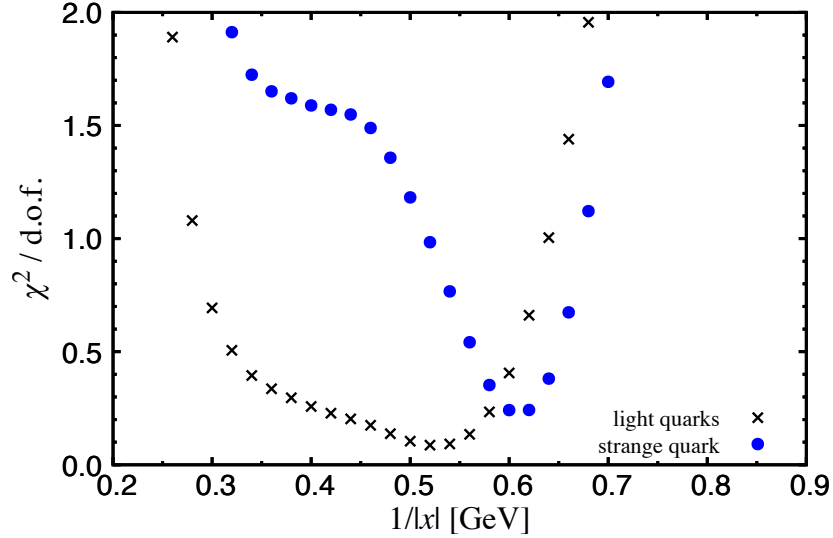


FIG. 7. The $\chi^2/\text{d.o.f.}$ obtained through the fit in the upper panel of Figure 5 (crosses) and in Figure 6 (circles).

chiral extrapolations are done by the fit function (30) with the substitution $\hat{m}_{ud}^{\overline{\text{MS}}} \rightarrow \hat{m}_s^{\overline{\text{MS}}}$. A plateau is seen in the same region as in the result for the light quarks mass.

Figure 7 shows the $\chi^2/\text{d.o.f.}$ obtained through the simultaneous fit both for the light (crosses) and strange (circles) quark masses. While the position-space renormalization fac-

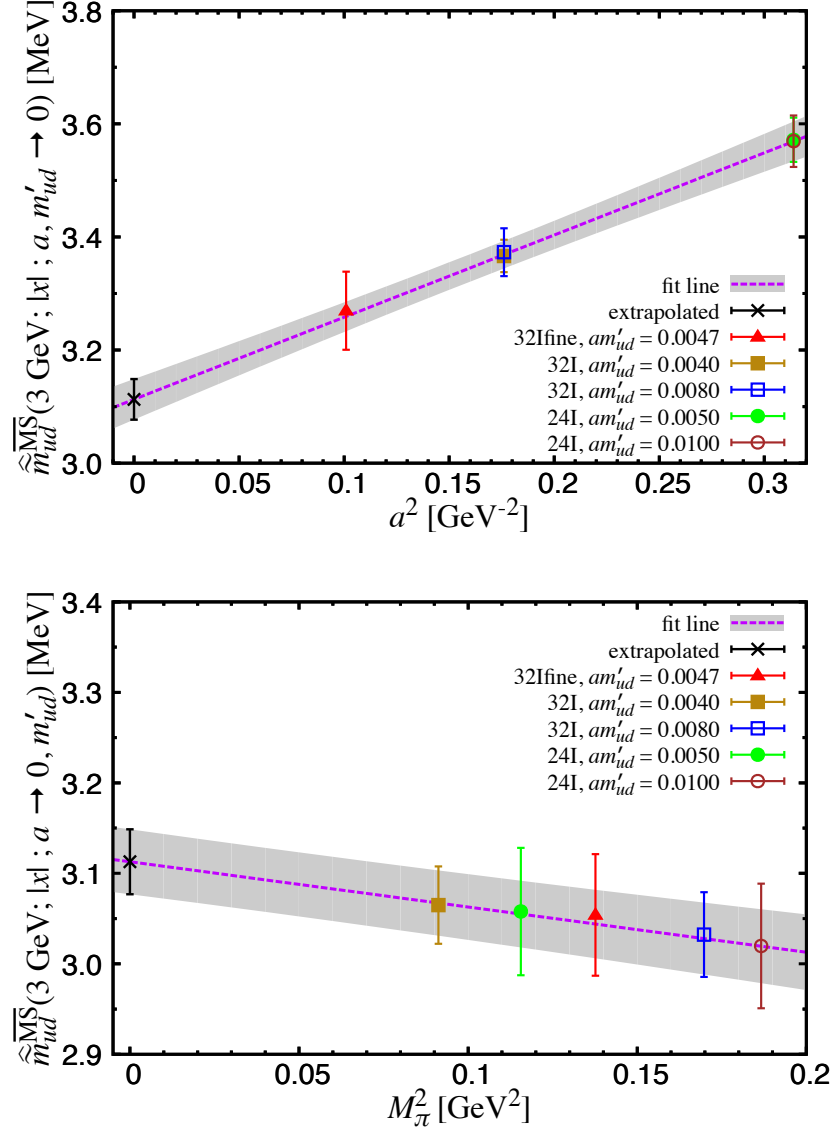


FIG. 8. Continuum and chiral extrapolations seen on the planes with $M_\pi = 0$ (upper panel) and $a = 0$ (lower panel) at $1/|x| = 0.52$ GeV.

tors calculated on each ensemble are uncorrelated, the statistical errors for Z_q and $m_q^{\text{bare}, 32\text{I}}$, which are taken from Ref. [16] and used in Eq. (26) to calculate unrenormalized quark mass $m_q^{\text{bare}}(1/a)$ for each lattice cutoff, are likely correlated. We interpret the small values of $\chi^2/\text{d.o.f.}$ shown in Figure 6 as resulting from our ignorance of such correlations. Since $\chi^2/\text{d.o.f.}$ at $1/|x| \simeq 0.6$ GeV, which roughly corresponds to $|x| \simeq 3a$ on the coarsest ensemble, is not too large, we may conclude that the spherical average does not suffer significantly from higher orders of $O(a)$ errors for $|x| \gtrsim 3a$.

To investigate the a - and M_π -dependences of $\hat{\bar{m}}_{ud}^{\overline{\text{MS}}}(3 \text{ GeV}; |x|; a, m'_{ud})$ more clearly, we visualize this extrapolation by analyzing the renormalized mass at a specific distance $|x|$ in the chiral limit

$$\begin{aligned}\hat{\bar{m}}_{ud}^{\overline{\text{MS}}}(3 \text{ GeV}; |x|; a, m'_{ud} \rightarrow 0) &\equiv \hat{\bar{m}}_{ud}^{\overline{\text{MS}}}(3 \text{ GeV}; |x|; a, m'_{ud}) - C_m M_\pi(a, m'_{ud})^2 \\ &= \hat{\bar{m}}_{ud}^{\overline{\text{MS}}}(3 \text{ GeV}; |x|) + C_a a^2,\end{aligned}\tag{31}$$

and in the continuum limit

$$\begin{aligned}\hat{\bar{m}}_{ud}^{\overline{\text{MS}}}(3 \text{ GeV}; |x|; a \rightarrow 0, m'_{ud}) &\equiv \hat{\bar{m}}_{ud}^{\overline{\text{MS}}}(3 \text{ GeV}; |x|; a, m'_{ud}) - C_a a^2 \\ &= \hat{\bar{m}}_{ud}^{\overline{\text{MS}}}(3 \text{ GeV}; |x|) + C_m M_\pi(a, m'_{ud})^2,\end{aligned}\tag{32}$$

with the parameters $\hat{\bar{m}}_{ud}^{\overline{\text{MS}}}(3 \text{ GeV}; |x|)$, $C_a(|x|)$ and $C_m(|x|)$ obtained through the simultaneous fit Eq. (30). Figure 8 shows the result for these values with the lines of the extrapolation at $1/|x| = 0.52 \text{ GeV}$. The result indicates both of the a - and M_π -dependences are treated well with their quadratic terms.

We use the result from the extrapolation including the data on the coarsest lattice to determine the renormalized quark mass. We estimate the central value of the quark mass at $1/|x| = 0.52 \text{ GeV}$, where $\chi^2/\text{d.o.f}$ is minimum. Our result is

$$m_{ud}^{\overline{\text{MS}}}(3 \text{ GeV}) = 3.113(36)(52)(24)(70) \text{ MeV}.\tag{33}$$

The first error is the statistical error. The second error is the systematic error due to discretization effects, which is estimated by increasing $1/|x|$ up to 0.60 GeV where a deviation from the plateau is beginning. The third error is the systematic uncertainty due to the truncation of the perturbative calculation, which is estimated by varying the parameter μ_x^* in the region $\mu_x^{*,\text{opt}}/\sqrt{2} \leq \mu_x^* \leq \sqrt{2}\mu_x^{*,\text{opt}}$. The forth error corresponds to the systematic error due to the uncertainty of the strong coupling constant, which is estimated by varying the scale of three-flavor QCD in the region $315 \text{ MeV} \leq \Lambda_{\text{QCD}}^{\overline{\text{MS}}} \leq 349 \text{ MeV}$ [18]. The result is compatible with our previous RBC/UKQCD result $m_{ud}^{\overline{\text{MS}}}(3 \text{ GeV}) = 2.997(49) \text{ MeV}$ [16] obtained through the RI/SMOM scheme using the same lattice ensembles and with the FLAG average $m_{ud}^{\overline{\text{MS}}}(3 \text{ GeV}) = 3.054(72) \text{ MeV}$ [13] of many works done through various renormalization procedures including the RI/(S)MOM and the Schrödinger functional [30] methods using $2 + 1$ -flavor ensembles. Applying the same procedure, we obtain the strange

TABLE III. Values of $\hat{Z}_m^{\overline{\text{MS}}/\text{lat}}(3 \text{ GeV}, 1/a; |x|; m'_{ud}) = 1/\hat{Z}_{P+S}^{\overline{\text{MS}}/\text{lat}}(3 \text{ GeV}, 1/a; |x|; m'_{ud})$ calculated on each ensemble at $1/|x| = 0.44 \text{ GeV}$, 0.52 GeV and 0.60 GeV . The given uncertainties (from left to right) are statistical, one from truncation of the perturbative calculation and one from $\Lambda_{\text{QCD}}^{\overline{\text{MS}}}$.

Ensemble set	m'_{ud}	$1/ x \text{ [GeV]}$		
		0.44	0.52	0.60
24I	0.0050	1.495(6)(25)(51)	1.553(5)(12)(35)	1.595(4)(7)(26)
	0.0100	1.467(2)(24)(50)	1.537(2)(12)(35)	1.584(2)(7)(26)
32I	0.0040	1.475(7)(25)(51)	1.511(5)(12)(34)	1.549(4)(7)(25)
	0.0080	1.446(11)(24)(50)	1.496(9)(12)(34)	1.542(7)(7)(25)
32Ifine	0.0047	1.456(9)(24)(50)	1.478(6)(11)(33)	1.498(4)(7)(24)

quark mass

$$m_s^{\overline{\text{MS}}}(3 \text{ GeV}) = 85.07(84)(1.33)(66)(1.92) \text{ MeV}, \quad (34)$$

which is also compatible with the FLAG average $m_s^{\overline{\text{MS}}}(3 \text{ GeV}) = 83.3(1.9) \text{ MeV}$ [13] and our previous RBC/UKQCD result $m_s^{\overline{\text{MS}}}(3 \text{ GeV}) = 81.64(1.17) \text{ MeV}$ [16] determined through the RI/SMOM scheme using the same ensembles.

In Table III, we summarize the quark mass renormalization factors calculated on each ensemble and at three values of $|x|$. The three errors shown (from left to right) correspond to the statistical error, the systematic error due to the truncation of the perturbative calculation and due to the uncertainty of the QCD scale $\Lambda_{\text{QCD}}^{\overline{\text{MS}}}$, in order. The latter two uncertainties, which are associated with perturbation theory, are more significant at longer distances as one can easily expect. As we have mentioned throughout the paper, we need to fix $|x|$ when we renormalize a quantity and take its continuum and chiral limits since the structure of a - and m'_{ud} -dependences depends on $|x|$.

VII. CONCLUSION

We have proposed a spherical averaging technique for position-space renormalization to reduce discretization errors and enhance the renormalization window. This technique has the further important advantage that it allows renormalized quantities to be defined at

any fixed physical distance. This allows a direct matching between renormalized quantities defined on ensembles with different lattice spacings and a continuum limit to be easily taken for position-space renormalized quantities at a fixed, physical renormalization scale.

The technique is applied to the quark mass renormalization using the scalar and pseudoscalar correlators in position space. We investigate the $|x|$ -dependence of the renormalized quark mass in the continuum limit and find a plateau even when the $\overline{\text{MS}}$ renormalized quark mass at finite a still depends slightly on the distance $|x|$ at which the intermediate position-space scheme is applied. The investigation of the $\chi^2/\text{d.o.f.}$ found for the continuum and chiral extrapolations implies that the a -dependence of sphere-averaged correlator is mostly $O(a^2)$ in the region $|x| \gtrsim 3a$. The renormalized quark mass obtained through this renormalization procedure agrees with the FLAG average and our previous RBC/UKQCD result obtained by using the RI/SMOM renormalization scheme on the same lattice ensembles.

The averaging approach proposed here is one of many possible schemes that can be devised which involve a smearing or averaging over lattice points in position space. However, the scheme proposed here may be of particular value because it involves two quite sharply defined scales: a long-distance scale $|x|$, the radius of the sphere over which we average, and a short-distance scale, the lattice spacing a which describes the thickness of the spherical shell of points which are averaged. The multi-linear interpolation method which is employed might be viewed as among the simplest prescriptions for creating this average. Having two such distinct scales may improve the continuum limit of the quantities renormalized using this method.

Since this X-space scheme is gauge invariant and free from contact terms, it prevents the mixing with irrelevant operators, which can be a serious complication for gauge-noninvariant schemes such as the RI/MOM scheme. Therefore, this position-space renormalization is especially well-suited for the four-quark operators in the $\Delta S = 1$ weak Hamiltonian where it can be imposed at the relatively long distances needed to define three-flavor operators — distances much longer than the Compton wavelength of the charm quark. At such distances (or at the corresponding energies below 1 GeV), the RI/MOM scheme is plagued by gauge noise and the usually justified neglect in the RI/MOM scheme of additional dimension-six operators constructed from a product of quark bilinears and gluon fields is likely to be a poor approximation. In fact, one of the motivations for this X-space method is to allow the Wilson coefficients of the three-flavor $\Delta S = 1$ weak Hamiltonian to be determined non-

perturbatively in terms of the more accurate, perturbatively-determined Wilson coefficients of the corresponding four-flavor theory.

Further technique must be developed before such a complete three-to-four flavor matching is possible. Some renormalization conditions can be imposed on the position-space two-point functions of four-quark operators renormalized in analogy with the sphere average of the two-point functions of scalar or pseudo-scalar currents presented in this paper. However, such in a position-space scheme, we will also need to constrain other Green's functions such as three-point functions of a four-quark operator and two two-quark operators to uniquely define a position-space scheme. The two-point functions of N mixing operators, will form a real symmetric matrix and allow at most $N(N+1)/2$ renormalization conditions to be imposed. These will be insufficient to determine the needed $N \times N$ renormalization matrix. An extension of the spherical averaging procedure to such three-point functions is the next step with is being developed.

ACKNOWLEDGMENTS

The authors thank their RBC and UKQCD colleagues for many useful discussions especially Peter Boyle and Robert Mawhinney. This work is supported in part by the US DOE grant #de-sc0011941.

Appendix A: Irregular a -dependence of spherical average

Since the interpolation Eq. (14) contains $n_\mu = \lfloor x_\mu/a \rfloor$, which is a discontinuous function of x/a , some irregularity could occur and the continuum extrapolation with only a term proportional to a^2 may not be accurate. In this Appendix, we discuss the significance of such irregular a -dependence of the spherical average.

Let us begin with the case of one dimension, in which the interpolated value $\bar{f}(x)$ of a quantity $f(x)$ defined in Eq. (10) can be written as

$$\bar{f}_a(x) = F(x) + c_a(x)a^2 + \frac{x^2 F''(x)}{2} \left(\frac{a}{x}(n+1) - 1 \right) \left(1 - \frac{a}{x}n \right) + O(a^3). \quad (\text{A1})$$

Here, $F''(x)$ stands for the second derivative of $F(x)$ and $c_a(x)$ comes from $c_{a,n}$ and $c_{a,n+1}$ in Eq. (9), which are the discretization errors in the values $f_{a,n}$ and $f_{a,n+1}$ evaluated on the lattice. We omit the possible logarithmic a -dependence of $F(x)$ and $F''(x)$ for simplicity.

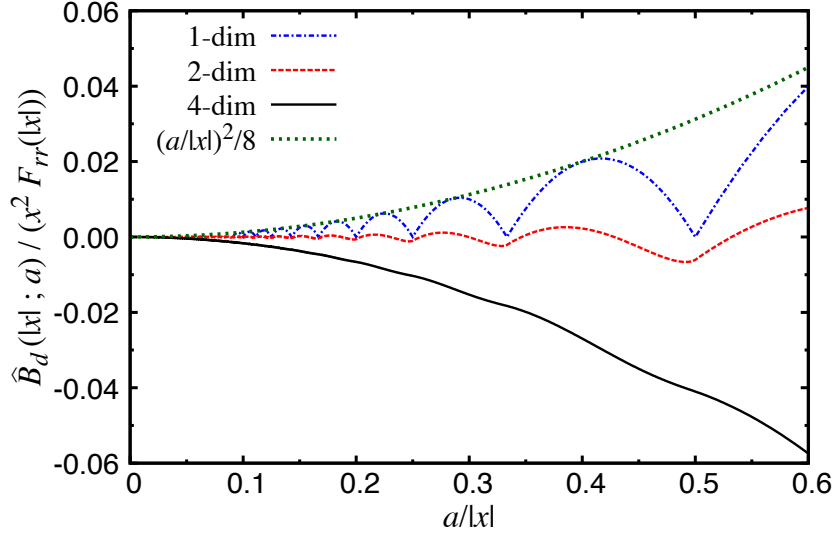


FIG. 9. $B_1(x; a)/(x^2 F''(x))$, $\hat{B}_2(|x|; a)/(x^2 F_{rr}(|x|))$ and $\hat{B}_4(|x|; a)/(x^2 F_{rr}(|x|))$ plotted as functions of $a/|x|$. The curve of $(a/|x|)^2/8$ is also plotted for comparison.

While the both of the second and third terms in Eq. (A1) are expected to contain complicated a -dependence, the third term

$$B_1(x; a) = \frac{x^2 F''(x)}{2} \left(\frac{a}{x} (n+1) - 1 \right) \left(1 - \frac{a}{x} n \right), \quad (\text{A2})$$

can be explicitly analyzed and therefore is discussed first. Since the value of $n = \lfloor x/a \rfloor$ jumps where x/a is an integer, the a -dependence of $I_1(x; a)/(x^2 F''(x))$ given by Eq. (A2) is drawn (dashed curve) in Figure 9. Thus, the continuum extrapolation with a few data points with an assumption of simple a^2 discretization error could be inaccurate. While such ambiguity is expected to be less than 1% of $x^2 F''(x)$ in the case of one dimension, one could imagine that in higher dimensions the spherical average further softens such irregular dependence on a and makes the continuum extrapolation more accurate.

The interpolation in d dimensions can be written as

$$\bar{f}_a(x) = F(x) + c_a(x) a^2 + B_d(x; a) + O(a^3), \quad (\text{A3})$$

where

$$B_d(x; a) = \frac{x^2}{2} \sum_{\mu=1}^d F_{\mu\mu}(x) \left(\frac{a}{|x|} (n_\mu + 1) - \frac{x_\mu}{|x|} \right) \left(\frac{x_\mu}{|x|} - \frac{a}{|x|} n_\mu \right), \quad (\text{A4})$$

and $F_{\mu\mu}(x)$ is the second derivative of $F(x)$ with respect to x_μ . Averaging over the sphere by the integral given in Eq. (12) for two dimensions or in Eq. (16) for four dimensions, this

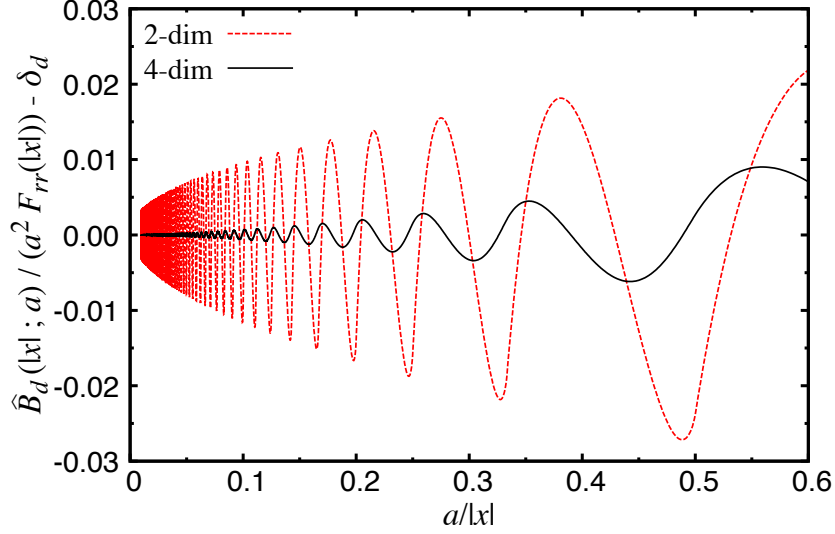


FIG. 10. $B_2(|x|; a)/(a^2 F_{rr}(|x|))$ and $B_4(|x|; a)/(a^2 F_{rr}(|x|))$ shifted by δ_d , the mid point of the oscillation. Note by dividing by a^2 instead of by $|x|^2$ as is done in Figure 9, we are plotting the correction relative to the regular a^2 error.

term becomes

$$\begin{aligned} \hat{B}_d(|x|; a) = C_d x^2 \int_0^{\pi/2} d\theta \sin^{d-2} \theta \left(F_{rr}(|x|) \cos^2 \theta + \frac{F_r(|x|)}{|x|} \sin^2 \theta \right) \\ \times \left(\frac{a}{|x|} \left(\left\lfloor \frac{|x|}{a} \cos \theta \right\rfloor + 1 \right) - \cos \theta \right) \left(\cos \theta - \frac{a}{|x|} \left\lfloor \frac{|x|}{a} \cos \theta \right\rfloor \right), \end{aligned} \quad (\text{A5})$$

where

$$C_2 = \frac{2}{\pi}, \quad C_4 = \frac{8}{\pi}, \quad (\text{A6})$$

and $F_r(|x|)$ and $F_{rr}(|x|)$ respectively stand for the first and second derivatives of $F(|x|)$ with respect to $|x|$.

In order to describe the a dependence implied by Eq. (A5), we need to assume a relation between the $F_{rr}(|x|)$ and $F_r(|x|)/|x|$ terms found in the first line of that equation. For the purposes of illustration we will assume that $F(|x|)$, which in this application is expected to be a slowly varying function of $|x|$, behaves as $\ln(|x|)$ so we can replace $F_r(|x|)$ by the $|x|F_{rr}(|x|)$. In this case, Eq. (A5) becomes

$$\begin{aligned} \hat{B}_d(|x|; a) \simeq C_d x^2 F_{rr}(|x|) \int_0^{\pi/2} d\theta \sin^{d-2} \theta (2 \cos^2 \theta - 1) \\ \times \left(\frac{a}{|x|} \left(\left\lfloor \frac{|x|}{a} \cos \theta \right\rfloor + 1 \right) - \cos \theta \right) \left(\cos \theta - \frac{a}{|x|} \left\lfloor \frac{|x|}{a} \cos \theta \right\rfloor \right). \end{aligned} \quad (\text{A7})$$

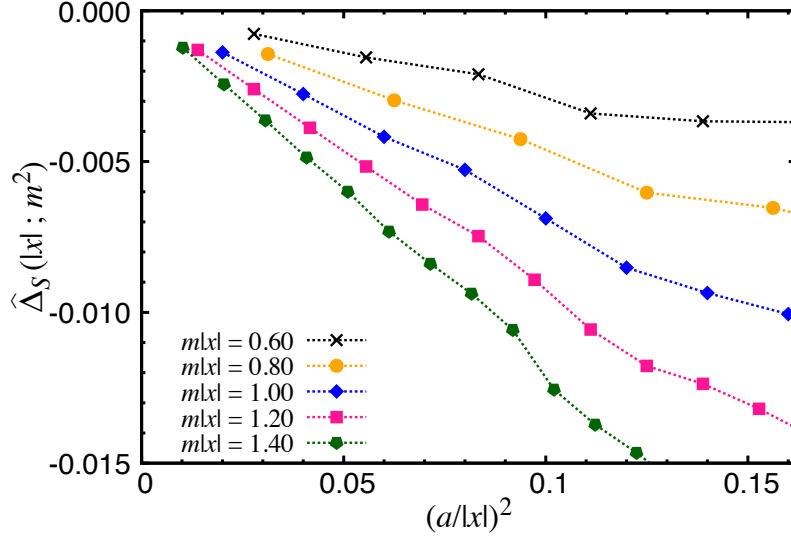


FIG. 11. $\hat{\Delta}_S(|x|; m^2)$ versus $(a/|x|)^2$ for several values of $m|x|$.

Figure 9 also shows the results for the spherical average $\hat{B}_d(|x|; a)$ normalized by $x^2 F_{rr}(|x|)$ in two and four dimensions. The magnitude of the irregular a -dependence in two dimensions is smaller than that in one dimension and therefore the continuum extrapolation with a regular a^2 term is expected to be more accurate. The irregular a -dependence of the spherical average in four dimensions is even smaller than that in two dimensions in the sense explained below. The significance of the irregular term in

$$\frac{\hat{B}_d(|x|; a)}{x^2 F_{rr}(|x|)} = \delta_d \cdot (a/|x|)^2 + (\text{irregular oscillation}) + O((a/|x|)^3), \quad (\text{A8})$$

can be investigated by

$$\frac{\hat{B}_d(|x|; a)}{a^2 F_{rr}(|x|)} - \delta_d, \quad (\text{A9})$$

which is plotted in Figure 10 for two and four dimensions. Here, we find $\delta_2 \simeq 0.00047$ and $\delta_4 \simeq 0.16667$. As the figure indicates, the irregular oscillation in four dimensions is even smaller than that in two dimensions. It means the continuum limit can be safely taken with a regular a^2 term.

Thus, we conclude that the irregular a -dependence associated with the third term of Eq. (A1) or (A3) is negligible. We proceed to discuss the other source of the irregular

a -dependence associated with $c_a(x)$ in Eq. (A1) or (A3), which can be written as

$$c_a(x) = a^{-4} \sum_{i,j,k,l=0}^1 \Delta_{1,i} \Delta_{2,j} \Delta_{3,k} \Delta_{4,l} c_{a,n+i\hat{1}+j\hat{2}+k\hat{3}+l\hat{4}}, \quad (\text{A10})$$

in the case of four dimensions. Here, c_n for the scalar or pseudoscalar correlator may be roughly approximated to a dispersion integral of the difference between the lattice and continuum propagators of a scalar field

$$c_{a,n} a^2 = \int_0^\infty ds \rho(s) \delta D_F(an; s), \quad (\text{A11})$$

$$\delta D_F(an; m^2) = D_F^{\text{lat}}(an; m^2) - D_F^{\text{cont}}(an; m^2), \quad (\text{A12})$$

$$D_F^{\text{lat}}(an; m^2) = \int_{-\pi/a}^{\pi/a} \frac{d^4 q}{(2\pi)^4} e^{iaqn} \frac{1}{4a^{-2} \sum_\mu \sin^2 \frac{aq_\mu}{2} + m^2}, \quad (\text{A13})$$

$$D_F^{\text{cont}}(x; m^2) = \int_{-\infty}^\infty \frac{d^4 q}{(2\pi)^4} e^{iqx} \frac{1}{q^2 + m^2} = \frac{m}{4\pi^2} \frac{K_1(m|x|)}{|x|}, \quad (\text{A14})$$

where $\rho(s)$ is the corresponding spectral function and $K_1(z)$ is the modified Bessel function of the second kind. To quantify the significance of c_n , we analyze the spherical average $\hat{\Delta}_S(|x|; m^2)$ of

$$\Delta_S(an; m^2) = \frac{\delta D_F(an; m^2)}{D_F^{\text{cont}}(x; m^2)|_{x=an}}. \quad (\text{A15})$$

The result is shown in Figure 11, which indicates that the discretization error is mostly proportional to a^2 for $|x| \gtrsim 3a$ and that the continuum extrapolation using lattice data at $|x| \simeq 3a, 4a$ and $5a$ is likely accurate within the $O(0.1\%)$ level.

While the above analysis using the bosonic propagator may be valid in QCD at long distances, the discretization error of Green's functions in the perturbative regime may need to be discussed in terms of fermionic propagators. We analyze the spherical average $\hat{\Delta}_{2f}(|x|; 0)$ of

$$\Delta_{2f}(an; 0) = \lim_{m \rightarrow 0} \frac{G_S^{\text{lat,free}}(an; m) - G_S^{\text{cont,free}}(x; m)}{G_S^{\text{cont,free}}(x; m)} \Big|_{x=an}, \quad (\text{A16})$$

$$G_S^{\text{cont,free}}(x; m) = \frac{3}{\pi^4 x^6}, \quad (\text{A17})$$

$$G_S^{\text{lat,free}}(x; m) = \text{Tr} \left[S_F^{\text{lat,free}}(x; m) S_F^{\text{lat,free}}(-x; m) \right], \quad (\text{A18})$$

where the lattice propagator $S_F^{\text{lat,free}}(an; m)$ in free field theory at small input mass $am \lesssim 0.1$ is quite sensitive to finite volume since the physical length scale in the deconfinement phase is associated with the input quark mass, not the pion mass. Here, we calculate it

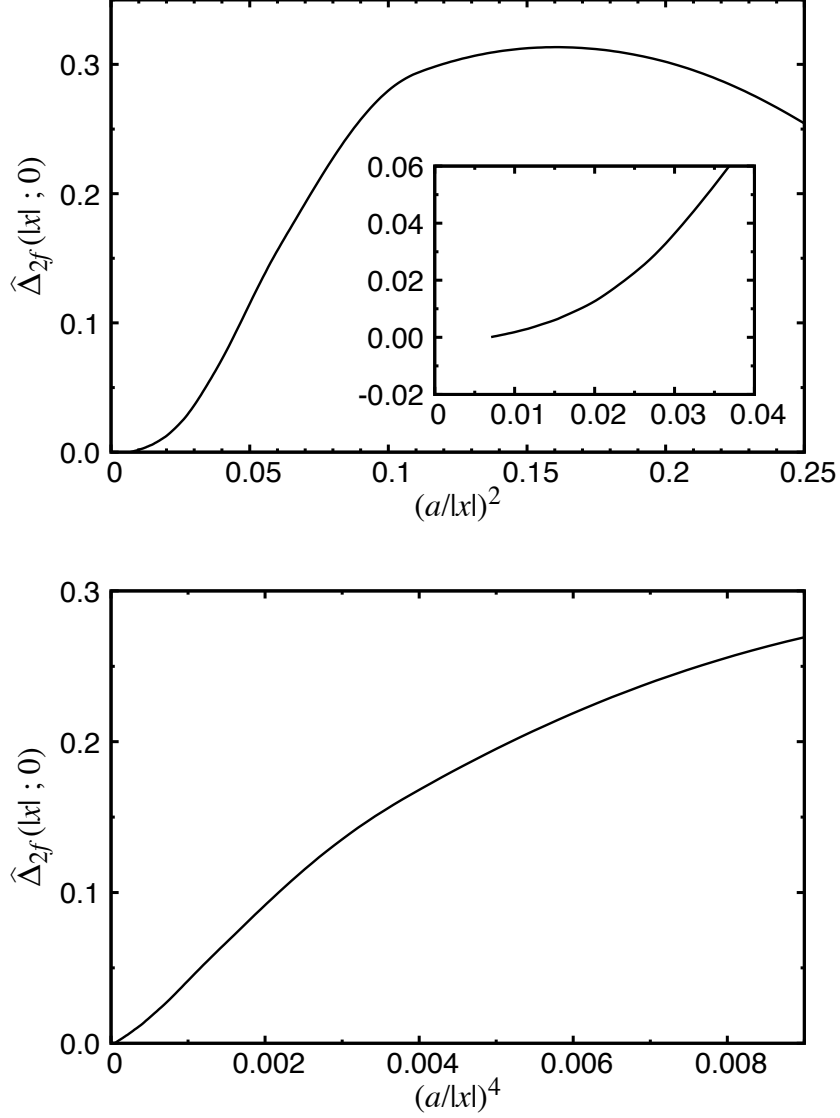


FIG. 12. $\hat{\Delta}_{2f}(|x|; 0)$ as a function of $(a/|x|)^2$ (upper panel) and $(a/|x|)^4$ (lower panel).

as the Fourier transform of the corresponding momentum-space propagator of domain-wall fermions [22, 31]. The calculation on a 200^4 lattice at $am \sim 0.005$ still suffers from significant finite volume effects, which can mostly be estimated as the effect of the fermions wrapping around the volume in the continuum theory. See [11] for more detail. Figure 12 shows the result for the spherical average $\hat{\Delta}_{2f}(|x|; 0)$ plotted as a function of $(a/|x|)^2$ (upper panel) and $(a/|x|)^4$ (lower panel). Although the a -dependence at small values of a appears to be proportional to a^4 , the coefficient is somehow large $\sim 50(a/|x|)^4$. We might therefore need to be careful when we take the continuum limit. Of course, nonperturbative interactions

could reduce the magnitude of the $O(a^4)$ term to a size closer to that found above using the bosonic propagator.

-
- [1] G. Martinelli, G. C. Rossi, C. T. Sachrajda, S. R. Sharpe, M. Talevi, and M. Testa, “Nonperturbative improvement of composite operators with Wilson fermions,” *Phys. Lett. B* **411** (1997) 141–151, [arXiv:hep-lat/9705018 \[hep-lat\]](#).
 - [2] V. Gimenez, L. Giusti, S. Guerriero, V. Lubicz, G. Martinelli, S. Petrarca, J. Reyes, B. Taglienti, and E. Trevigne, “Non-perturbative renormalization of lattice operators in coordinate space,” *Phys. Lett. B* **598** (2004) 227–236, [arXiv:hep-lat/0406019 \[hep-lat\]](#).
 - [3] G. Martinelli, C. Pittori, C. T. Sachrajda, M. Testa, and A. Vladikas, “A General method for nonperturbative renormalization of lattice operators,” *Nucl. Phys. B* **445** (1995) 81–108, [arXiv:hep-lat/9411010 \[hep-lat\]](#).
 - [4] M. Luscher, P. Weisz, and U. Wolff, “A Numerical method to compute the running coupling in asymptotically free theories,” *Nucl. Phys. B* **359** (1991) 221–243.
 - [5] K. Jansen, C. Liu, M. Luscher, H. Simma, S. Sint, R. Sommer, P. Weisz, and U. Wolff, “Nonperturbative renormalization of lattice QCD at all scales,” *Phys. Lett. B* **372** (1996) 275–282, [arXiv:hep-lat/9512009 \[hep-lat\]](#).
 - [6] **RBC, UKQCD** Collaboration, R. Arthur and P. A. Boyle, “Step Scaling with off-shell renormalisation,” *Phys. Rev. D* **83** (2011) 114511, [arXiv:1006.0422 \[hep-lat\]](#).
 - [7] K. Cichy, K. Jansen, and P. Korcyl, “Non-perturbative running of renormalization constants from correlators in coordinate space using step scaling,” *Nucl. Phys. B* **913** (2016) 278–300, [arXiv:1608.02481 \[hep-lat\]](#).
 - [8] K. Symanzik, “Continuum Limit and Improved Action in Lattice Theories. 1. Principles and ϕ^4 Theory,” *Nucl. Phys. B* **226** (1983) 187–204.
 - [9] K. Symanzik, “Continuum Limit and Improved Action in Lattice Theories. 2. $O(N)$ Nonlinear Sigma Model in Perturbation Theory,” *Nucl. Phys. B* **226** (1983) 205–227.
 - [10] K. Cichy, K. Jansen, and P. Korcyl, “Non-perturbative renormalization in coordinate space for $N_f = 2$ maximally twisted mass fermions with tree-level Symanzik improved gauge action,” *Nucl. Phys. B* **865** (2012) 268–290, [arXiv:1207.0628 \[hep-lat\]](#).
 - [11] **JLQCD** Collaboration, M. Tomii, G. Cossu, B. Fahy, H. Fukaya, S. Hashimoto, T. Kaneko,

- and J. Noaki, “Renormalization of domain-wall bilinear operators with short-distance current correlators,” *Phys. Rev.* **D94** no. 5, (2016) 054504, [arXiv:1604.08702 \[hep-lat\]](#).
- [12] K. G. Chetyrkin and A. Maier, “Massless correlators of vector, scalar and tensor currents in position space at orders α_s^3 and α_s^4 : Explicit analytical results,” *Nucl. Phys.* **B844** (2011) 266–288, [arXiv:1010.1145 \[hep-ph\]](#).
- [13] S. Aoki *et al.*, “Review of lattice results concerning low-energy particle physics,” *Eur. Phys. J.* **C77** no. 2, (2017) 112, [arXiv:1607.00299 \[hep-lat\]](#).
- [14] Y. Aoki *et al.*, “Non-perturbative renormalization of quark bilinear operators and B(K) using domain wall fermions,” *Phys. Rev.* **D78** (2008) 054510, [arXiv:0712.1061 \[hep-lat\]](#).
- [15] C. Sturm, Y. Aoki, N. H. Christ, T. Izubuchi, C. T. C. Sachrajda, and A. Soni, “Renormalization of quark bilinear operators in a momentum-subtraction scheme with a nonexceptional subtraction point,” *Phys. Rev.* **D80** (2009) 014501, [arXiv:0901.2599 \[hep-ph\]](#).
- [16] **RBC, UKQCD** Collaboration, T. Blum *et al.*, “Domain wall QCD with physical quark masses,” *Phys. Rev.* **D93** no. 7, (2016) 074505, [arXiv:1411.7017 \[hep-lat\]](#).
- [17] M. C. Chu, J. M. Grandy, S. Huang, and J. W. Negele, “Correlation functions of hadron currents in the QCD vacuum calculated in lattice QCD,” *Phys. Rev.* **D48** (1993) 3340–3353, [arXiv:hep-lat/9306002 \[hep-lat\]](#).
- [18] **ParticleDataGroup** Collaboration, M. Tanabashi *et al.*, “Review of Particle Physics,” *Phys. Rev.* **D98** no. 3, (2018) 030001.
- [19] P. A. Baikov, K. G. Chetyrkin, and J. H. Kuhn, “Quark Mass and Field Anomalous Dimensions to $\mathcal{O}(\alpha_s^5)$,” *JHEP* **10** (2014) 76, [arXiv:1402.6611 \[hep-ph\]](#).
- [20] P. A. Baikov, K. G. Chetyrkin, and J. H. Kühn, “Five-Loop Running of the QCD coupling constant,” *Phys. Rev. Lett.* **118** no. 8, (2017) 082002, [arXiv:1606.08659 \[hep-ph\]](#).
- [21] D. B. Kaplan, “A Method for simulating chiral fermions on the lattice,” *Phys. Lett.* **B288** (1992) 342–347, [arXiv:hep-lat/9206013 \[hep-lat\]](#).
- [22] Y. Shamir, “Chiral fermions from lattice boundaries,” *Nucl. Phys.* **B406** (1993) 90–106, [arXiv:hep-lat/9303005 \[hep-lat\]](#).
- [23] Y. Iwasaki and T. Yoshie, “Renormalization Group Improved Action for SU(3) Lattice Gauge Theory and the String Tension,” *Phys. Lett.* **143B** (1984) 449–452.
- [24] Y. Iwasaki, “Renormalization Group Analysis of Lattice Theories and Improved Lattice

- Action: Two-Dimensional Nonlinear $O(N)$ Sigma Model,” *Nucl. Phys.* **B258** (1985) 141–156.
- [25] **RBC, UKQCD** Collaboration, Y. Aoki *et al.*, “Continuum Limit Physics from 2+1 Flavor Domain Wall QCD,” *Phys. Rev.* **D83** (2011) 074508, [arXiv:1011.0892 \[hep-lat\]](#).
- [26] **UKQCD** Collaboration, S. J. Hands, P. W. Stephenson, and A. McKerrell, “Point-to-point hadron correlation functions using the Sheikholeslami-Wohlert action,” *Phys. Rev.* **D51** (1995) 6394–6402, [arXiv:hep-lat/9412065 \[hep-lat\]](#).
- [27] G. ’t Hooft, “Computation of the Quantum Effects Due to a Four-Dimensional Pseudoparticle,” *Phys. Rev.* **D14** (1976) 3432–3450. [Erratum: *Phys. Rev.* **D18**, 2199 (1978)].
- [28] V. A. Novikov, M. A. Shifman, A. I. Vainshtein, and V. I. Zakharov, “Are All Hadrons Alike?,” *Nucl. Phys.* **B191** (1981) 301.
- [29] E. V. Shuryak, “Correlation functions in the QCD vacuum,” *Rev. Mod. Phys.* **65** (1993) 1–46.
- [30] M. Luscher, R. Narayanan, P. Weisz, and U. Wolff, “The Schrodinger functional: A Renormalizable probe for nonAbelian gauge theories,” *Nucl. Phys.* **B384** (1992) 168–228, [arXiv:hep-lat/9207009 \[hep-lat\]](#).
- [31] R. Narayanan and H. Neuberger, “Infinitely many regulator fields for chiral fermions,” *Phys. Lett.* **B302** (1993) 62–69, [arXiv:hep-lat/9212019 \[hep-lat\]](#).